Biosensors and Bioelectronics 257 (2024) 116339

Contents lists available at ScienceDirect

Biosensors and Bioelectronics

journal homepage: www.elsevier.com/locate/bios

Enhanced CRISPR/Cas12a-based quantitative detection of nucleic acids using double emulsion droplets

Yang Zhang [a,h], Hangrui Liu [b], Yuta Nakagawa [c], Yuzuki Nagasaka [c], Tianben Ding [c], Shi-Yang Tang [d], Yaxiaer Yalikun [e], Keisuke Goda [c,f,g], Ming Li [a,h,*]

[a] School of Engineering, Faculty of Science and Engineering, Macquarie University, Sydney, NSW 2109, Australia
[b] Department of Bioengineering and Therapeutic Sciences, University of California San Francisco, San Francisco, CA, 94158, USA
[c] Department of Chemistry, The University of Tokyo, Tokyo, 113-0033, Japan
[d] School of Electronics and Computer Science, University of Southampton, Southampton, SO17 1BJ, UK
[e] Division of Materials Science, Nara Institute of Science and Technology, 630-0192, Ikoma, Japan
[f] Department of Bioengineering, University of California, Los Angeles, CA, 90095, USA
[g] Institute of Technological Sciences, Wuhan University, Hubei, 430072, China
[h] School of Mechanical and Manufacturing Engineering, University of New South Wales, Sydney, NSW, 2052, Australia

ARTICLE INFO

Keywords:
CRISPR/Cas 12a based detection
Droplet microfluidics
Double emulsion droplets
DNA quantification

ABSTRACT

Pairing droplet microfluidics and CRISPR/Cas12a techniques creates a powerful solution for the detection and quantification of nucleic acids at the single-molecule level, due to its specificity, sensitivity, and simplicity. However, traditional water-in-oil (W/O) single emulsion (SE) droplets often present stability issues, affecting the accuracy and reproducibility of assay results. As an alternative, water-in-oil-in-water (W/O/W) double emulsion (DE) droplets offer superior stability and uniformity for droplet digital assays. Moreover, unlike SE droplets, DE droplets are compatible with commercially available flow cytometry instruments for high-throughput analysis. Despite these advantages, no study has demonstrated the use of DE droplets for CRISPR-based nucleic acid detection. In our study, we conducted a comparative analysis to assess the performance of SE and DE droplets in quantitative detection of human papillomavirus type 18 (HPV18) DNA based on CRISPR/Cas12a. We evaluated the stability of SEs and DEs by examining size variation, merging extent, and content interaction before and after incubation at different temperatures and time points. By integrating DE droplets with flow cytometry, we achieved high-throughput and high-accuracy CRISPR/Cas12a-based quantification of target HPV18 DNA. The DE platform, when paired with CRISPR/Cas12a and flow cytometry techniques, emerges as a reliable tool for absolute quantification of nucleic acid biomarkers.

1. Introduction

Droplet microfluidics has rapidly become a promising tool for detecting and quantifying nucleic acids, which are crucial biomarkers for disease diagnosis and treatment (Chen et al. 2021, 2022; Lathia et al., 2023; Prince et al., 2022; Sun et al., 2022; Teh et al., 2008; Zhang et al., 2013). Unlike traditional bulk assays which measure average signals across large populations, droplet microfluidics uncovers individual variations by isolating samples into distinct droplets (Chen et al., 2021; Prince et al., 2022; Si et al., 2020; Teh et al., 2008). This compartmentalization into uniform picolitre droplets offers multiple advantages, especially when quantifying rare and low-abundance targets (Collins et al., 2015; Liu et al., 2020). The confined small volume ensures a faster reaction between the molecules of interest and reagents, enhancing the assay's sensitivity and efficiency (Beer et al., 2008; Chen et al., 2022). Additionally, the reduced droplet size means less sample and reagent volume is consumed, leading to cost savings, and making the method more accessible for clinical diagnostics. Furthermore, precise encapsulation of nucleic acid molecules within these microdroplets enables single-molecule level detection of target genomes (Isozaki et al., 2020; Li et al., 2018a).

Droplet microfluidics has been paired with several traditional methods, such as polymerase chain reaction (PCR) (Olmedillas-López et al., 2022), loop-mediated isothermal amplification (LAMP) (Bageritz and Raddi, 2019; Bioćanin et al., 2019), and recombinase polymerase amplification (RPA) (Liu et al., 2022), to achieve single-molecule

* Corresponding author. School of Mechanical and Manufacturing Engineering, University of New South Wales, Sydney, NSW, 2052, Australia.
E-mail address: ming.li3@unsw.edu.au (M. Li).

https://doi.org/10.1016/j.bios.2024.116339
Received 4 March 2024; Received in revised form 5 April 2024; Accepted 24 April 2024
Available online 26 April 2024

nucleic acid detection. Yet, these methodologies have inherent limitations. The design of primers is intricate, often labor-intensive, and prone to non-specific amplification. This can inadvertently result in false-positive outcomes (Gerasimova and Kolpashchikov, 2014). Recently, the spotlight has turned to CRISPR/Cas12a-based nucleic acid detection, because of its simplicity, precision, and sensitivity (Gong et al., 2021; Gootenberg et al., 2017; Li et al., 2019; Liang et al., 2021; Tsou et al., 2020). When target DNA aligns with CRISPR-related RNA (crRNA) sequence, the non-specific cleavage activity of Cas12a protein is triggered, degrading the synthetic single-strand DNA reporter (ssDNA) adorned with quenched fluorescent oligo (Dronina et al., 2022; Wu et al., 2022b). Since its debut in 2017 (Li et al., 2018b), CRISPR/Cas12a technology has been a game-changer in molecular diagnostics, pinpointing specific gene segments for disease detection (Chen et al., 2018; Katti et al., 2022). Many studies have combined CRISPR/Cas12a with droplet microfluidics to detect and quantify target nucleic acids, such as plasmids and viral DNA/RNA, in rare and low-abundance samples (Calhoun et al., 2022; Gootenberg et al., 2017; Luo et al., 2022; Thakku et al., 2021; Wu et al., 2022b; Xue et al., 2022). However, conventional water-in-oil (W/O) single emulsion (SE) droplets employed for CRISPR/Cas12a-based nucleic acid detection can become unstable during complex incubation steps, like thermal cycling, heating, and shaking (Uberbacher et al., 2019; Wang et al., 2021). While several strategies, including the addition of surfactants (Cheng et al., 2021; Cowell et al., 2022), have been implemented to enhance droplet stability, SE droplets remain susceptible to coalescence and fragmentation. These shortcomings can lead to quantification inaccuracies and compromised partitions, reducing the sensitivity and efficiency of nucleic acid assays (Joensson and Andersson Svahn, 2012; Zhao, 2013).

Water-in-oil-in-water (W/O/W) double emulsion (DE) droplets are a promising alternative by dispersing W/O (SE) in a continuous aqueous phase (Brower et al., 2020b; Calhoun et al., 2022; Cowell et al., 2022; Zhang et al., 2013). The oil shell of DE droplets encases the inner aqueous phase, which contains both reagents and target nucleic acids, granting added protection against coalescence (Khariton et al., 2023; Cowell et al., 2022). As a result, DE droplets exhibit higher monodispersity and uniformity than SE droplets, facilitating individual droplet reactions and minimizing contamination (Cowell et al., 2022). Unlike SE droplets, which are inclined to merge, DE droplets, even when slightly ruptured, tend to release their inner content into the outer aqueous phase. This released content can then be efficiently processed at the downstream. Additionally, W/O/W DE droplets suspended in an aqueous solution are well-suited for commercially available flow cytometry (FC) instruments, allowing for high-throughput screening. While there have been studies using FC to screen various cell lines encapsulated in DE droplets (Brower et al., 2020b; Li et al., 2021; Liu et al., 2021), no research has yet explored the synergy of DE and FC techniques, specifically for CRISPR-based nucleic acid detection.

In this study, we explored the partitioning capabilities of SE and DE droplets in the context of CRISPR/Cas12a-based single-molecule nucleic acid detection. We assessed and compared the structural stability, content mixing, and sample retention between SE and DE droplets. We also showcased flow cytometric screening of DE droplets containing CRISPR/Cas12a reaction for target HPV18 DNA quantification. To the best of our knowledge, this is the first time that the integration of CRISPR/Cas12a with DE droplets has been reported for high-throughput and high-accuracy quantification of nucleic acids.

2. Results and discussion

2.1. Workflow of CRISPR/Cas12a-based nucleic acid detection using SE and DE droplets

As schematically illustrated in Fig. 1, we integrated droplet microfluidics and CRISPR/Cas12a techniques to quantitatively detect target DNA at the single-molecule level. First, SE and DE droplets with a diameter of ~20 μm containing CRISPR/Cas12a reaction mixture were generated. A common T-junction droplet generator was used to generate SE droplets, while a two-layer microfluidic chip with spatial wettability patterning developed in our previous study (Liu et al., 2021) was used to generate DE droplets (see Fig. S1). Second, all generated droplets were collected in 1.5-mL centrifuge tubes and incubated at 37.5 °C for 30 min (Luo et al., 2022).

During the incubation, the designed crRNA can specifically bind with the target DNA sequences and activate nonspecific *trans*-cleavage activity of Cas12a proteins. The activated Cas12a proteins cut off surrounding fluorescein (FAM)-quencher ssDNA reporters to physically separate fluorophore from the quencher, resulting in the release of fluorescence and a detectable signal. Finally, both SE and DE droplets were transferred to glass slides for imaging under an inverted fluorescence microscope. Further, DE droplets suspended in an aqueous solution can be loaded into a commercially available flow cytometer for

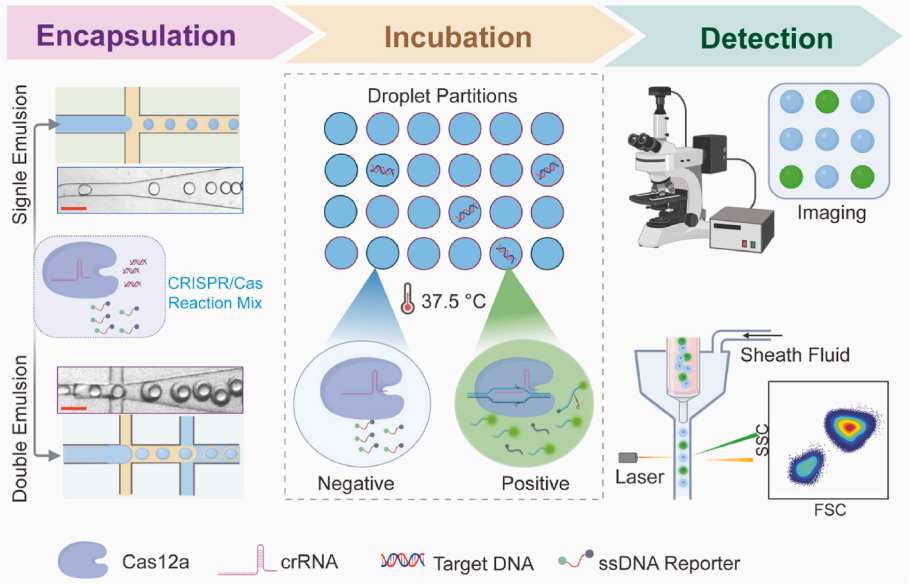

Fig. 1. Schematic diagram illustrating the workflow of CRISPR/Cas12a-based nucleic acid detection at the single-molecule level using SE and DE microdroplets. Scale bar is 50 μm.

high-throughput detection and quantification of target DNA.

2.2. DE droplets provide robust compartments

The stability of droplets significantly affects downstream processes, causing changes in droplet size and reducing emulsion uniformity (Wu et al., 2020). This impact is particularly critical in quantitative analysis of nucleic acid molecules, where accurate measurements are vital for determining the concentration of analytes within individual droplets. Variations in droplet size can lead to incorrect results by distorting the relationship between analyte concentration and the observed signals. We examined the stability of SE and DE droplets encapsulating CRISPR/Cas12a reaction mixture before and after incubation (at 37.5 °C for 30 min) under a microscope. Almost all DE droplets were found to maintain their structural integrity and monodispersity after incubation, while merged droplets (~20% of total population) with inconsistent sizes appeared in SE droplet samples (see Fig. 2a insets and Fig. S2). Although polydisperse droplet emulsions could be identified in downstream analysis, they lead to inconsistent quantification results. We further measured and compared the diameter of SE droplets and the inner diameter (ID) and outer diameter (OD) of DE droplets before and after incubation (Fig. 2a). The average diameter of SE droplets increased by 2.42%, from 16.910 ± 1.004 μm to 17.320 ± 1.412 μm, after incubation. In contrast, the ID and OD of DE droplets experienced a slight increase (less than 1.62% and 3.83%) from 19.002 ± 0.900 μm and 25.590 ± 0.840 μm to 19.310 ± 0.740 μm and 26.570 ± 0.920 μm, respectively.

To quantify the size variation of SE and DE droplets, we calculated the coefficient of size variation ratio (Δ) at different incubation temperatures and time points (Fig. 2b). Δ is defined as $\Delta Mean/Mean_0$, where ΔMean is the mean of the change in the diameter and $Mean_0$ is the mean of the initial diameter. The Δ of SE droplets exhibited a substantial ~3% increase as incubation time and temperature increased, whereas the Δ of ID of DE droplets was less than 0.15% across all conditions. Furthermore, we compared the standard deviation (SD) and the variation of SD (ΔSD) of the two groups (see Fig. S3), which indicate the dispersity degree of the data distribution around the average mean. The ΔSD of the diameter of SE droplets was not only higher than that of ID and OD of DE droplets but also showed a larger variation after incubation (SE: +40.6%; DE: 17% for ID and +9.5% for OD). This indicates that the size distribution of SE droplets is more dispersed than DE droplets due to merging and break-up. The slight increase, 1.6% in the ID and 3.8% in the OD of DE droplets after incubation, is largely due to the regulation of osmolarity across the inner and outer aqueous phases. The osmotic pressure within the inner phase slightly exceeds that of the outer phase due to the encapsulation of CRISPR-related reagents. Consequently, water would be transferred from the outer phase to the inner phase solution, resulting in the swelling of droplets (Zhuang et al., 2023).

2.3. DE droplets reduce sample loss

It is challenging to analyze clinical samples with limited sample volumes, especially when absolute quantitative analysis is critical (Cheng et al., 2022; Wu et al., 2022a). However, sample loss is inevitable in commonly used droplet microfluidic platforms due to incomplete encapsulation, droplet merging, phase diffusion, and droplet breakup (Chung et al., 2017). To examine the sample loss during incubation, SE, and DE droplets with the same size (~20 μm) containing CRISPR/Cas12a reaction mixture were generated. Afterwards, ~100 μL of SE

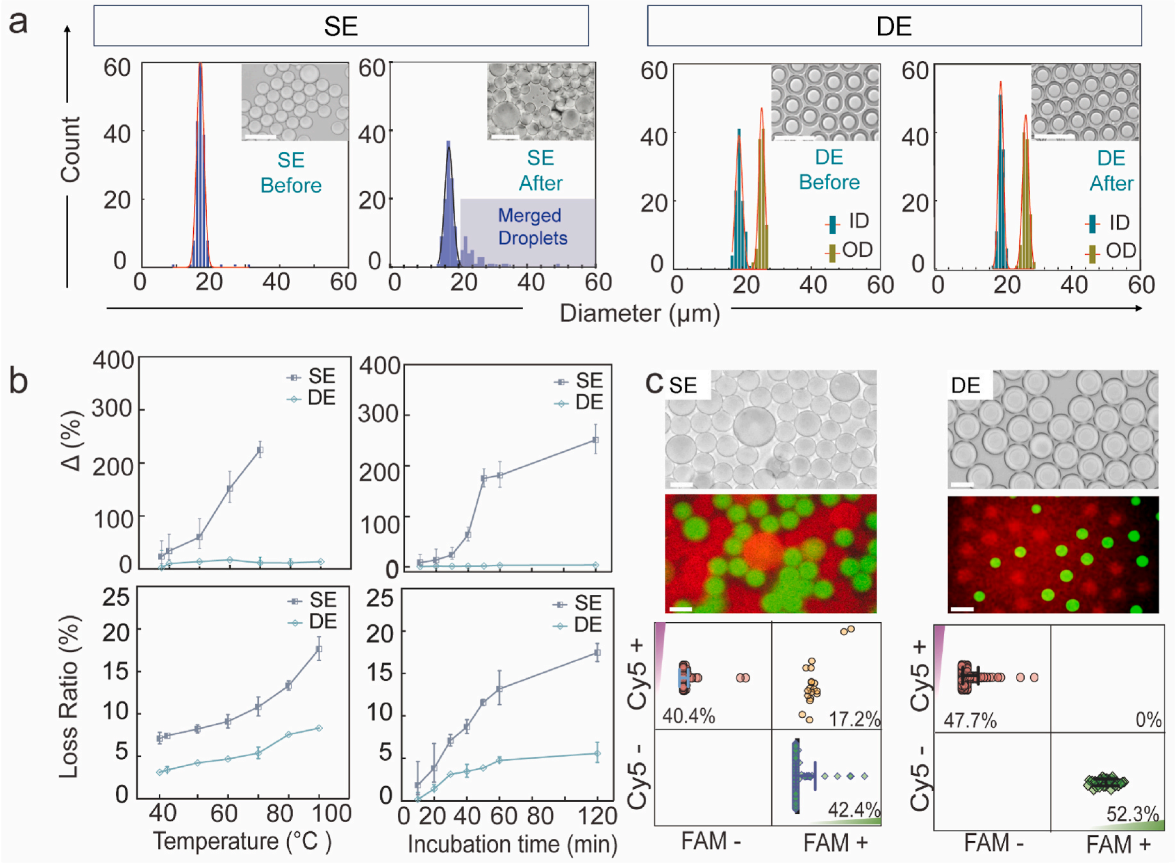

Fig. 2. Changes in the diameters of SE and DE droplets after incubation. (a) The distribution of the diameters of SE and DE droplets after incubation at 37.5 °C for 30 min; (b) Changes in the average droplet diameter and sample loss ratio at different temperatures ranging from 37.5 °C to 90 °C and different incubation time ranging from 0 to 120 min. Scale bars are 50 μm; (c). Images (top) and scatter plots (bottom) showing the mixing degree for SE and DE droplets. Scale bars are 20 μm.

and DE droplets each were collected in separate tubes and incubated at 37.5 °C for 30 min (Fig. S4). A portion of SE droplets were found to experience rupture and diffusion after incubation, causing the release of the encapsulated aqueous phase.

The concentration of leaked DNA reporters from SE and DE droplets after incubation was determined using calibration curves (Fig. S5), which were built from the fluorescence intensity of known dilutions of activated CRISPR/Cas12a solution in nuclease-free water (NFW) and outer phase solution of DEs (PBS with surfactants), respectively. For fluorescence intensity measurements, the uppermost aqueous layer in the tube containing SE droplets was diluted in 100 μL NFW, while 100 μL of upper aqueous phase was extracted from the tube containing DE droplets. Herein, we calculated the sample loss ratios at different incubation times and temperatures to assess the capability of SE and DE to confine target molecules. Across three replicates, SE droplets were shown to have larger sample loss ratio than DE droplets in all conditions, i.e., different incubation times ranging from 0 min to 120 min and different incubation temperatures ranging from 37.5 °C to 90 °C (Fig. 2b). In addition, the impact of droplet volume and differences in oil phase solutions on sample loss was studied in Section 3 of **Supplementary Information**.

2.4. DE droplets avoid content mixing

Droplet microfluidic techniques for absolute quantification of target molecules are based on the partitioning of a bulk sample into millions of microdroplets containing only one single target molecule. Since the number of droplets containing target molecules is used to calculate the absolute concentration of target in the original sample, the ability to partition samples within physically isolated droplet emulsions is important for high-precision analysis (D'Agostino et al., 2023; Cowell et al., 2022; Jiang et al., 2023). To compare the content compartmentalization ability of SE and DE droplets, we introduced two ssDNA reporters which induce fluorescence signals within two different wavelength bands, Cy5 (red) and FAM (green), when Cas12a is activated (see Fig. S6). Two groups of SE and DE droplets containing either Cy5 or FAM reporters were prepared separately and then 100 μL of each group were mixed in one tube at a 1:1 (v/v) ratio. After incubating at 37.5 °C for 30 min, we captured images of the mixed droplet samples (see Fig. 2c top)

In the case of SE droplets, we observed some droplets exhibiting a vibrant orange colour, indicating the presence of both Cy5 and FAM fluorescence reporters inside the same droplets. Additionally, some droplets with unchanged diameters showing orange fluorescence were noticeable, possibly due to content diffusion between droplets during incubation. This content exchange between different SE droplets leads to invalid partitions in quantification analysis. In contrast, DE droplets are robust enough to effectively maintain their compartmentalization during incubation, and there were no DE droplets containing two different reporters that were observed. To quantitatively examine the degree of content mixing for SE and DE droplets, about 1000 droplets in each group were imaged and their fluorescence intensity were measured (Fig. 2c bottom). The results showed that 17.2% of SE droplets contained both Cy5 and FAM reporters after incubation, while no DE droplets contained both. Therefore, DE droplets can fully compartmentalize contents and prevent inner cores from merging, which are important for sensitive and quantitative detection of low-abundance biomarkers.

2.5. Integration of DE droplets and flow cytometry for high-throughput CRISPR-based nucleic acid quantification

Since DE droplets suspended in an aqueous solution are compatible with standard flow cytometry (FC) instruments (Brower et al. 2020a, 2020b; Li et al., 2021), they can be used as an effective method for carrying out ultra-sensitive and high-throughput nucleic acid detection based on CRISPR/Cas12a (Fozouni et al., 2021; Yue et al., 2021). To demonstrate the ability of integrated DE-FC technique for target DNA quantification, CRISPR reaction mixture without target DNA and the one with 100 nM target DNA were encapsulated separately in ~20 μm DE droplets to obtain negative and positive control populations, respectively. The positive and negative droplets were also mixed at different ratios and after CRISPR reaction, a commercially available FC was used to screen these mixed droplet samples (Fig. 3a).

We first detected positive droplets encapsulating the mixture of CRISPR reaction and target HPV18 dsDNA (Fig. 3b). Although relatively low fluorescence signals were detected from negative DE droplets (i.e., without the target DNA), two control groups were clearly distinguishable by gating based on forward scatter height (FSC–H) and side scatter height (SSC–H). Here, FSC and SSC signals were related to the size and the complexity or granularity of the DEs, respectively. The detailed gating strategy is shown in Fig. S7. The median fluorescence intensity of the gated positive droplet population was roughly ten times higher than that of the negative population, where the intensity was 4.9×10^5 and 5.6×10^4 a.u., respectively.

To evaluate the efficacy of our established workflow for quantifying nucleic acids, we prepared four mock samples to simulate varying concentrations of target HPV 18 DNA by mixing positive and negative DE droplets at different volume ratios. The fraction of positive droplets (FPD) was determined by counting droplets in each mixed group of a total of 1000 events, resulting in proportions of 5%, 31%, 54%, and 72% (Fig. 3c). The relationship between the FPD and the sample concentration can be built using Poisson distribution (**Supplementary Information, Section 4**). In addition, more than 10,000 DE droplets from each group were loaded into FC and detected within less than 2 min. Two distinct groups for positive and negative droplets were found in all the cases, and FPDs were counted to be 4.5%, 31.8%, 55.3% and 70.8% (Fig. 3c). These FC results were in good agreement with the ones obtained from microscopy (Fig. 3d).

Furthermore, our integrated DE-FC approach enabled HPV18 DNA detection at the single-molecule level (Fig. S10b) and the quantification of target DNA with low concentrations as 10 fM (Fig. S10a). We noted that no detectable signals of positive droplets were found for samples containing non-target DNA (Fig. S11), and there exists an excellent linear relationship between actual HPV18 concentrations in artificial urine and measured values. These results indicated the sensitivity, specificity, and robustness of our developed approach for the detection and quantification of HPV DNA in complex biofluids.

3. Materials and methods

More information is provided in the Supporting Information.

4. Conclusion

In this study, the usage of DE droplets presents several advantages over SE droplets for quantitative detection of nucleic acids, such as excellent structural stability as well as negligible sample loss and content mixing. These features are important for preventing contamination, maintaining partition integrity, and ensuring the accuracy of droplet digital assays. In addition, DE droplets are compatible with flow cytometry techniques, thus allowing high-throughput quantification of target HPV DNA with high sensitivity and specificity at a constant temperature. Our study provides a highly versatile and valuable tool for absolute nucleic acid quantification in various fields of research. It is expected to lead to breakthroughs in droplet digital assays, enhancement in disease diagnosis, monitoring, and treatment, as well as a better understanding of biological and chemical processes.

CRediT authorship contribution statement

Yang Zhang: Writing – original draft, Visualization, Validation, Software, Project administration, Methodology, Investigation, Formal

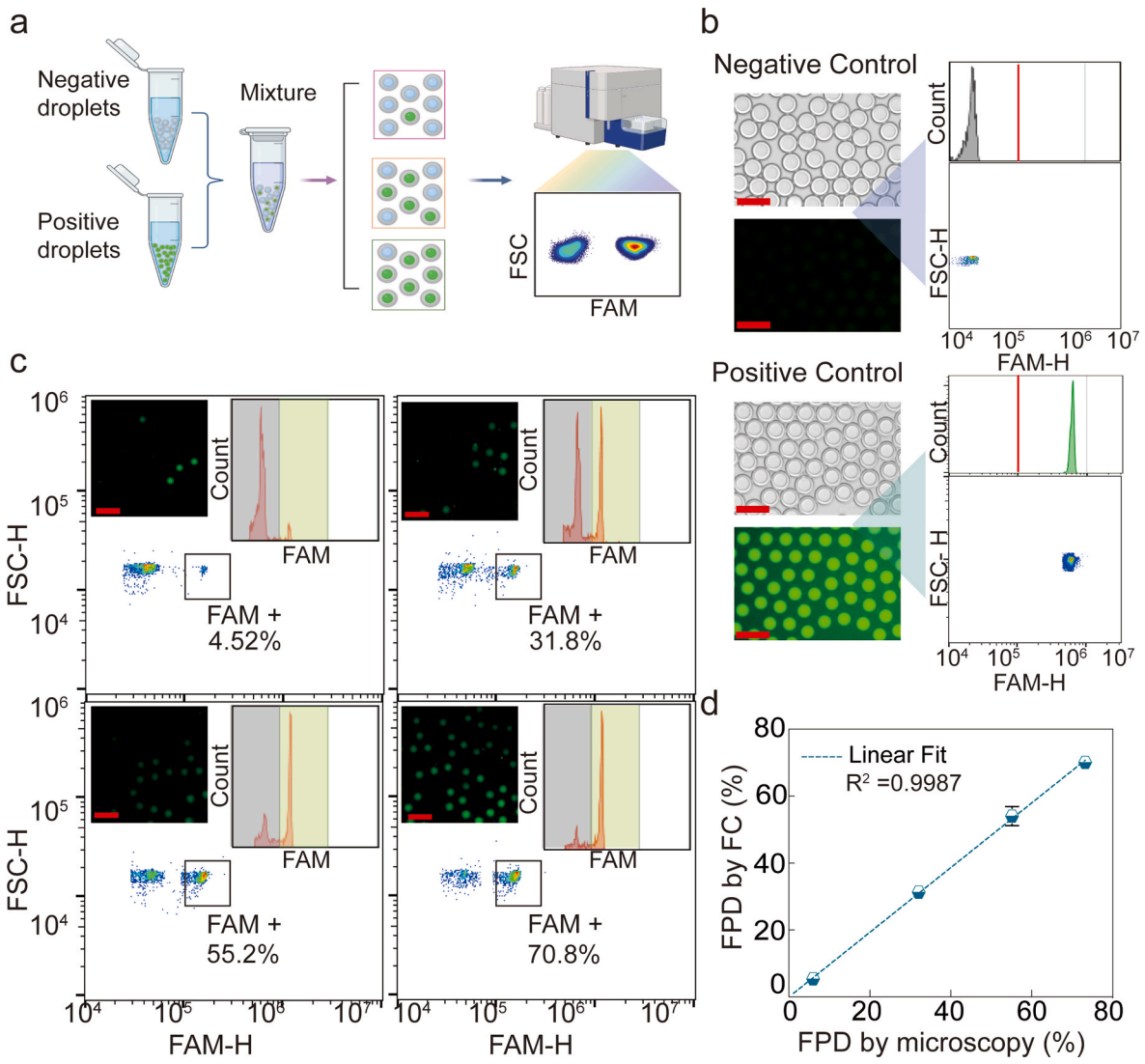

Fig. 3. Integration of DE droplets with flow cytometry for CRISPR/Cas12a-based detection and quantification of nucleic acids. (a) Workflow of integrating DE droplets with flow cytometry for target quantification; (b) Flow cytometry detection of positive (with target) and negative (without target) DE droplets; (c) Flow cytometry quantification of different DE populations containing positive and negative droplets mixed in different ratios. Scale bars are 50 μm. (d) Linear relationship between the FPD obtained from microscopy images and measured by flow cytometry.

analysis, Data curation. **Hangrui Liu:** Methodology. **Yuta Nakagawa:** Writing – review & editing. **Yuzuki Nagasaka:** Writing – review & editing. **Tianben Ding:** Writing – review & editing. **Shi-Yang Tang:** Writing – review & editing, Funding acquisition. **Yaxiaer Yalikun:** Writing – review & editing. **Keisuke Goda:** Writing – review & editing. **Ming Li:** Conceptualization, Methodology, Validation, Resources, Writing – original draft, Writing – review & editing, Visualization, Supervision, Project administration, Funding acquisition.

Declaration of competing interest

The authors declare that they have no known competing financial interests or personal relationships that could have appeared to influence the work reported in this paper.

Data availability

Data will be made available on request.

Acknowledgments

This research is supported mainly by the Australian Research Council (ARC) Discovery Project (DP200102269) and partly by the JSPS Core-to-Core Program. Ming Li is a recipient of the National Health and Medical Research Council (NHMRC) Emerging Leadership Fellowship (GNT2017679). Yang Zhang acknowledges the financial support from International Macquarie Research Excellence Scholarship (iMQRES) at Macquarie University for graduate study. Fig. 1 was created with BioRender.com.

Appendix A. Supplementary data

Supplementary data to this article can be found online at https://doi.org/10.1016/j.bios.2024.116339.

References

Bageritz, J., Raddi, G., 2019. Single Cell Methods: Sequencing and Proteomics, vols. 73–85.

Beer, N.R., Wheeler, E.K., Lee-Houghton, L., Watkins, N., Nasarabadi, S., Hebert, N., Leung, P., Arnold, D.W., Bailey, C.G., Colston, B.W., 2008. Anal. Chem. 80 (6), 1854–1858.
Biočanin, M., Bues, J., Dainese, R., Amstad, E., Deplancke, B., 2019. Lab Chip 19 (9), 1610–1620.
Brower, K.K., Carswell-Crumpton, C., Klemm, S., Cruz, B., Kim, G., Calhoun, S.G.K., Nichols, L., Fordyce, P.M., 2020a. Lab Chip 20 (12), 2062–2074.
Brower, K.K., Khariton, M., Suzuki, P.H., Still 2nd, C., Kim, G., Calhoun, S.G.K., Qi, L.S., Wang, B., Fordyce, P.M., 2020b. Anal. Chem. 92 (19), 13262–13270.
Calhoun, S.G.K., Brower, K.K., Suja, V.C., Kim, G., Wang, N., McCully, A.L., Kusumaatmaja, H., Fuller, G.G., Fordyce, P.M., 2022. Lab Chip 22 (12), 2315–2330.
Chen, J.S., Ma, E., Harrington, L.B., Da Costa, M., Tian, X., Palefsky, J.M., Doudna, J.A., 2018. Science 360 (6387), 436–439.
Chen, Z., Kheiri, S., Gevorkian, A., Young, E.W., Andre, V., Deisenroth, T., Kumacheva, E., 2021. Lab Chip 21 (20), 3952–3962.
Chen, Z., Kheiri, S., Young, E.W.K., Kumacheva, E., 2022. Langmuir 38 (20), 6233–6248.
Cheng, G., Lin, K.-T., Ye, Y., Jiang, H., Ngai, T., Ho, Y.-P., 2021. ACS Appl. Mater. Interfaces 13 (18), 21914–21923.
Cheng, X., Li, Y., Kou, J., Liao, D., Zhang, W., Yin, L., Man, S., Ma, L., 2022. Biosensors Bioelectron 215, 114559.
Chung, M.T., Núñez, D., Cai, D., Kurabayashi, K., 2017. Lab Chip 17 (21), 3664–3671.
Collins, D.J., Neild, A., deMello, A., Liu, A.-Q., Ai, Y., 2015. Lab Chip 15 (17), 3439–3459.
Cowell, T.W., Dobria, A., Han, H.-S., 2022. ACS Appl. Mater. Interfaces 14 (18), 20528–20537.
D'Agostino, C., Preziosi, V., Caiazza, G., Maiorino, M.V., Fridjonsson, E., Guido, S., 2023. Soft Matter 19 (17), 3104–3112.
Dronina, J., Samukaite-Bubniene, U., Ramanavicius, A., 2022. J. Nanobiotechnol. 20 (1), 41.
Fozouni, P., Son, S., Díaz de León Derby, M., Knott, G.J., Gray, C.N., D'Ambrosio, M.V., Zhao, C., Switz, N.A., Kumar, G.R., Stephens, S.I., Boehm, D., Tsou, C.-L., Shu, J., Bhuiya, A., Armstrong, M., Harris, A.R., Chen, P.-Y., Osterloh, J.M., Meyer-Franke, A., Joehnk, B., Walcott, K., Sil, A., Langelier, C., Pollard, K.S., Crawford, E. D., Puschnik, A.S., Phelps, M., Kistler, A., DeRisi, J.L., Doudna, J.A., Fletcher, D.A., Ott, M., 2021. Cell 184 (2), 323–333.e329.
Gerasimova, Y.V., Kolpashchikov, D.M., 2014. Chem. Soc. Rev. 43 (17), 6405–6438.
Gong, J., Zhang, G., Wang, W., Liang, L., Li, Q., Liu, M., Xue, L., Tang, G., 2021. Sci. Rep. 11 (1), 12800.
Gootenberg, J.S., Abudayyeh, O.O., Lee, J.W., Essletzbichler, P., Dy, A.J., Joung, J., Verdine, V., Donghia, N., Daringer, N.M., Freije, C.A., 2017. Science 356 (6336), 438–442.
Isozaki, A., Nakagawa, Y., Loo, M.H., Shibata, Y., Tanaka, N., Setyaningrum, D.L., Park, J.-W., Shirasaki, Y., Mikami, H., Huang, D., Tsoi, H., Riche, C.T., Ota, T., Miwa, H., Kanda, Y., Ito, T., Yamada, K., Iwata, O., Suzuki, K., Ohnuki, S., Ohya, Y., Kato, Y., Hasunuma, T., Matsusaka, S., Yamagishi, M., Yazawa, M., Uemura, S., Nagasawa, K., Watarai, H., Di Carlo, D., Goda, K., 2020. Sci. Adv. 6 (22), eaba6712.
Jiang, Z., Shi, H., Tang, X., Qin, J., 2023. TrAC, Trends Anal. Chem. 159, 116932.
Joensson, H.N., Andersson Svahn, H., 2012. Angew. Chem. Int. Ed. 51 (49), 12176–12192.
Katti, A., Diaz, B.J., Caragine, C.M., Sanjana, N.E., Dow, L.E., 2022. Nat. Rev. Cancer 22 (5), 259–279.
Khariton, M., McClune, C.J., Brower, K.K., Klemm, S., Sattely, E.S., Fordyce, P.M., Wang, B., 2023. Anal. Chem. 95 (2), 935–945.
Lathia, R., Nampoothiri, K.N., Sagar, N., Bansal, S., Modak, C.D., Sen, P., 2023. Langmuir 39 (7), 2461–2482.
Li, M., Liu, H., Zhuang, S., Goda, K., 2021. RSC Adv. 11 (34), 20944–20960.
Li, M., van Zee, M., Riche, C.T., Tofig, B., Gallaher, S.D., Merchant, S.S., Damoiseaux, R., Goda, K., Di Carlo, D., 2018a. Small 14 (44), e1803315.
Li, S.-Y., Cheng, Q.-X., Liu, J.-K., Nie, X.-Q., Zhao, G.-P., Wang, J., 2018b. Cell Res. 28 (4), 491–493.
Li, Y., Li, S., Wang, J., Liu, G., 2019. Trends Biotechnol. 37 (7), 730–743.
Liang, Y., Lin, H., Zou, L., Zhao, J., Li, B., Wang, H., Lu, J., Sun, J., Yang, X., Deng, X., Tang, S., 2021. Microbiol. Spectr. 9 (3), e0101721.
Liu, F.X., Cui, J.Q., Park, H., Chan, K.W., Leung, T., Tang, B.Z., Yao, S., 2022. Anal. Chem. 94 (15), 5883–5892.
Liu, H., Li, M., Wang, Y., Piper, J., Jiang, L., 2020. Micromachines 11 (1), 94.
Liu, H., Piper, J.A., Li, M., 2021. Anal. Chem. 93 (31), 10955–10965.
Luo, X., Xue, Y., Ju, E., Tao, Y., Li, M., Zhou, L., Yang, C., Zhou, J., Wang, J., 2022. Anal. Chim. Acta 1192, 339336.
Olmedillas-López, S., Olivera-Salazar, R., García-Arranz, M., García-Olmo, D., 2022. Mol. Diagn. Ther. 26 (1), 61–87.
Prince, E., Kheiri, S., Wang, Y., Xu, F., Cruickshank, J., Topolskaia, V., Tao, H., Young, E. W., McGuigan, A.P., Cescon, D.W., 2022. Adv. Healthcare Mater. 11 (1), 2101085.
Si, H., Xu, G., Jing, F., Sun, P., Zhao, D., Wu, D., 2020. Sensors Actuators B: Chem. 318, 128197.
Sun, J., Lo, H.T.J., Fan, L., Yiu, T.L., Shakoor, A., Li, G., Lee, W.Y.W., Sun, D., 2022. Sci. Adv. 8 (33), eabp9245.
Teh, S.-Y., Lin, R., Hung, L.-H., Lee, A.P., 2008. Lab Chip 8 (2), 198–220.
Thakku, S.G., Ackerman, C.M., Myhrvold, C., Bhattacharyya, R.P., Livny, J., Ma, P., Gomez, G.I., Sabeti, P.C., Blainey, P.C., Hung, D.T., 2021. bioRxiv.
Tsou, J.H., Leng, Q.X., Jiang, F., 2020. Diagnostics 10 (2).
Uberbacher, C., Obergasteiger, J., Volta, M., Venezia, S., Muller, S., Pesce, I., Pizzi, S., Lamonaca, G., Picard, A., Cattelan, G., Malpeli, G., Zoli, M., Beccano-Kelly, D., Flynn, R., Wade-Martins, R., Pramstaller, P.P., Hicks, A.A., Cowley, S.A., Corti, C., 2019. Stem Cell Res. 41.
Wang, S., Li, H., Kou, Z., Ren, F., Jin, Y., Yang, L., Dong, X., Yang, M., Zhao, J., Liu, H., Dong, N., Jia, L., Chen, X., Zhou, Y., Qiu, S., Hao, R., Song, H., 2021. Clin. Microbiol. Infect. 27 (3), 443–450.
Wu, H., Cao, X., Meng, Y., Richards, D., Wu, J., Ye, Z., deMello, A.J., 2022a. Biosensors Bioelectron 211, 114377.
Wu, X., Chan, C., Springs, S.L., Lee, Y.H., Lu, T.K., Yu, H., 2022b. Anal. Chim. Acta 1196, 339494.
Wu, X., Lv, Q., Wu, Y., Li, C., Cen, K., 2020. Chem. Eng. Sci. 223, 115645.
Xue, Y., Luo, X., Xu, W., Wang, K., Wu, M., Chen, L., Yang, G., Ma, K., Yao, M., Zhou, Q., 2022. Anal. Chem.
Yue, H.H., Shu, B.W., Tian, T., Xiong, E.H., Huang, M.Q., Zhu, D.B., Sun, J., Liu, Q., Wang, S.C., Li, Y.R., Zhou, X.M., 2021. Nano Lett. 21 (11), 4643–4653.
Zhang, Y., Ho, Y.-P., Chiu, Y.-L., Chan, H.F., Chlebina, B., Schuhmann, T., You, L., Leong, K.W., 2013. Biomaterials 34 (19), 4564–4572.
Zhao, C.-X., 2013. Adv. Drug Del. Rev. 65 (11–12), 1420–1446.
Zhuang, S., Liu, H., Inglis, D.W., Li, M., 2023. Anal. Chem. 95 (3), 2039–2046.